



Dynamic characteristic reconfiguration of a fixture-workpiece system for vibration suppression in milling of thin-walled workpieces based on MR damping fixture

Junjin Ma¹ · Yunfei Li¹ · Dinghua Zhang² · Bo Zhao¹ · Xiaoyan Pang³

Received: 8 April 2022 / Accepted: 10 September 2022 / Published online: 16 September 2022
© The Author(s), under exclusive licence to Springer-Verlag London Ltd., part of Springer Nature 2022

Abstract

Milling of the low rigidity and large deformation thin-walled workpiece is a critical challenging task due to the obvious machining vibration, which greatly affects the machining accuracy and surface quality of the final part. Compared with the conventional vibration control methods, this paper mainly focuses on suppressing machining vibration by magnetorheological (MR) dampers in milling of the thin-walled workpiece. A novel dynamic characteristic reconstruction strategy of the fixture-workpiece system is proposed to improve the dynamic characteristics of the milling system considering the effect of material removal based on MR damping fixture. Then, the fixture-workpiece system dynamic characteristics reconstruction model is established, subsequently. The time-varying modal parameters in different conditions are iteratively identified, and the stable depth of cut is obtained at any moment. Based on this, the control currents of the MR damping fixture are calculated to offset the change of the damping and stiffness properties of the milling system, which is caused by material removal. Finally, the feasibility and effectiveness of the proposed method are validated by several experiments. Experimental results show that the dynamic properties of the fixture-workpiece system are reconstructed by the MR damping fixture compared with the initial machining state, the vibration response is reduced by 30 to approximately 70%, and the machined surface is improved effectively.

Keywords Machining vibration suppression · Dynamic characteristic reconstruction · Dynamic stability · Fixture design · Milling

1 Introduction

Milling plays an important role in the aerospace industry, which is widely used in machining of the low rigidity and large deformation workpieces such as aeroengine blades, casings, impellers, blisks, etc. However, the dynamic cutting force acting on the weakly rigid workpiece enhances the time-varying dynamic characteristics of milling system,

which caused the severe vibration response at different positions on the workpiece body in milling, so vibration is an obvious obstacle in obtaining higher machining accuracy, better surface integrity, and less tool wear [1, 2]. Therefore, it is necessary to investigate the dynamic characteristics evolution of the thin-walled workpiece-fixture system for suppressing vibration in milling.

Over the past few decades, for the efforts of investigating system dynamic characteristics to mitigate the vibration in milling of the thin-walled workpiece, there are mainly three kinds of methods: cutting parameters optimization, passive control method, and active control method. For the cutting parameter optimization, the analytical prediction method is used to evaluate the machining state [3], then, the reasonable cutting parameters can be selected. Yang et al. [4] proposed a new dynamic model of the tool-workpiece system to investigate the effect of varying workpiece dynamics on the stability in peripheral milling of thin-walled workpieces. Ding et al. [5] proposed a new system stability analysis method that can

✉ Junjin Ma
majhpu@hpu.edu.cn

¹ School of Mechanical and Power Engineering, Henan Polytechnic University, Jiaozuo 454000, China

² Key Laboratory of Contemporary Design and Integrated Manufacturing Technology, Ministry of Education, Northwestern Polytechnical University, Xi'an 710072, China

³ College of Computer Science and Technology, Henan Polytechnic University, Jiaozuo 454000, China

realize stable machining by variable spindle speed cutting method. Qin et al. [6] developed a novel milling stability prediction method based on Chebyshev wavelet to identify tool chatter, and the method is compared with the existing methods. Lou et al. [7] proposed a Cotes-formula-based stability prediction method and validated it by experiments. Dong and Qiu [8] proposed an updated numerical integration method, which is verified by machining tests. Li et al. [9] presented a stability prediction approach based on the Newton–Cotes rules, which suppressed chatter and improved the machining efficiency and surface quality of the workpiece. Shi et al. [10] derived a new computational model and obtained an updated frequency response function to analyze machining stability, which was verified by experiments. However, these methods mainly focus on how to control the calculation accuracy and speed. Furthermore, they can only be used for cutting parameters selection, which cannot enlarge the stability region and improve milling efficiency with material removal. In addition, this method cannot be widely applied due to the limitation of machining quality and NC equipment performance.

For the passive control method to pursue machining stability, process stiffness enhancement methods by clamping method, support rod, mass block, and material removal sequence are investigated by many researchers. Namazi et al. [11] analyzed the effect of contact stiffness and damping performance between tool shank and spindle on milling stability. Luo et al. [12] optimized machining allowance distribution and material removal sequence based on stability lobes for improving machining stability. In addition, Mori et al. [13] presented viscoelastic damper support for chatter suppression, and machining stability is obviously improved compared with other used methods by experiments. Fei et al. [14] proposed a moving fixture element method to suppress milling vibration, and the effectiveness of the fixture in the machining process was verified. Craig et al. [15] presented a novel fixture concept that used deformable flexure pins to fill the space between the workpiece and the locators to improve the stiffness of the workpiece. A support system using a pivot mechanism for suppressing vibration in thin-wall milling is designed by Matsubara et al. [16]. Then, Wang et al. [17] designed a special fixture using low shrinkage of low-melting-point alloy to clamp thin-walled parts to guarantee machining accuracy. From the above analysis, the existing process stiffness enhancement methods do not have the characteristics of adjustable support force and dynamic characteristics, and they cannot compensate for the spatiotemporal evolution of system dynamic characteristics, which caused by material removal and different dynamic processing positions.

For the active control method, system dynamic characteristic reconstruction by complex special fixture system [18], piezoelectric intelligent unit [19], and electromagnetic

actuator [20] are investigated in lots of works. With the development of sensing technology, signal recognition and intelligent materials, and active self-reconfiguration intelligent fixture system have become a research hotspot at present. Papastathis et al. [21] proposed a model which characterized the dynamic response between active fixture components and thin-walled workpieces under dynamic moving loads. Subsequently, Parus et al. [22] proposed an active control system considering the dampness to suppress regenerative chatter in the milling of the thin-walled workpiece. Considering the dynamic characteristics of a fixture to suppress machining vibration, Ransom et al. [23] designed a fixture system based on an eddy current damper to suppress machining vibration effectively. Greiner-Petter et al. [24] proposed a semi-active fluid mechanism based on variable stiffness damping using magnetorheological valves and springs. Moradi et al. [25, 26] designed an adjustable vibration absorber for chatter suppression in milling and proposed a nonlinear delay differential equation to describe the system-coupled dynamic model. Then, the position, stiffness, and damping parameters of the adjustable shock absorber were optimized. Similarly, Ma et al. [27] designed a MR flexible fixture for suppressing machining vibration in the milling of the thin-walled plate. Guo et al. [28] proposed a mechanical/magnetorheological composite clamping method for the milling process to avoid chatting, which was verified in the milling of thin-walled parts. From these, the methods are only applied to simple parts, and the stability of the milling system can be improved by regulating the stiffness and damping of the fixture-workpiece system. However, for the thin-walled workpiece, these methods need to design a special fixture system, paste mass block, and other auxiliary components and these methods are not adjustable under complex machining conditions.

Due to material removal in the milling of the thin-walled workpiece, cutting stage, and other factors, the time-varying dynamic characteristics of the fixture-workpiece system vary significantly, which causes machining instability, and the effect of the whole fixture properties to suppress vibration is investigated comprehensively in limited works. Consequently, to address this problem, a novel MR damping fixture is designed for milling of thin-walled parts, and the fixture has the controllable characteristics in damping and stiffness without changing the original fixture layout, which can reconstruct the dynamic characteristics of the fixture-workpiece system according to actual machining state. Then, an active control method based on MR damping fixture is proposed and validated. The remainder of this paper is organized as follows. Section 2 describes the dynamic characteristic reconstruction scheme of the fixture-workpiece system. Fixture-workpiece system dynamic characteristics reconstruction model is proposed, and the time-varying

modal parameters in different conditions are iteratively identified, then the control currents of the MR damping fixture are calculated to offset the change of damping and stiffness properties of the milling system caused by material removal, which is shown in Sect. 3. Subsequently, in Sect. 4, several experiments are conducted to validate the feasibility and efficiency of the proposed method. Finally, some conclusions are summarized.

2 Problem formulation

For the problem of vibration suppression caused by system dynamic characteristics evolution in the milling of the thin-walled workpiece, compared with conventional process parameter optimization and uncontrollable process stiffness enhancement, the proposed method using controllable MR dampers can reconstruct the dynamic characteristics of the fixture-workpiece system to improve the machining stability for suppressing vibration, and the schematic diagram is shown in Fig. 1.

Based on machining dynamics theory, when MR dampers have no effect on a thin-walled workpiece, the dynamic equation of the fixture-workpiece system is described by a n -dimensional equation:

$$M\ddot{q}(t) + C\dot{q}(t) + Kq(t) = F_z(t) \tag{1}$$

where M , C , and K denote mass, damping, and stiffness matrices of the original system. $\ddot{q}(t)$, $\dot{q}(t)$, and $q(t)$ are acceleration, velocity, and displacement vectors. $F_z(t)$ represents normal cutting force vector acting on the different cutting positions.

Considering the geometry of the thin-walled workpiece and its clamping constraints, the weak rigidity regions of the thin-walled workpiece are enforced using MR dampers, which can improve the dynamic stiffness and damping of the milling system. Then, the thin-walled workpiece-fixture system evolved into a statically indeterminate system. Therefore, the dynamic equation of the workpiece-fixture system after local modification can be rewritten as

$$M\ddot{q} + (C + C_f)\dot{q} + (K + K_f)q + P_z z = F_z(t) \tag{2}$$

where C_f and K_f denote the damping and stiffness matrices caused by MR dampers in the fixture. $P_z z$ is the hysteresis force produced by MR dampers.

With workpiece material removal, the dynamic characteristics of the fixture-workpiece system evolve continuously, which causes the stable boundary of the machining system decreases and gradually close to the unstable machining region. To ensure stable machining, the MR dampers are regulated by the external current to improve the dynamic damping and stiffness characteristics of the fixture-workpiece system. Then, for the reconstructed dynamic characteristics of the fixture-workpiece system with MR dampers, the dynamic equation of motion can be expressed as

$$(M + \Delta M)\ddot{q} + (C + \Delta C + C_f)\dot{q} + (K + \Delta K + K_f)q + P_z z = F_z(t) \tag{3}$$

where ΔM , ΔC , and ΔK are the change of modal mass, damping, and stiffness matrices of workpiece caused by material removal.

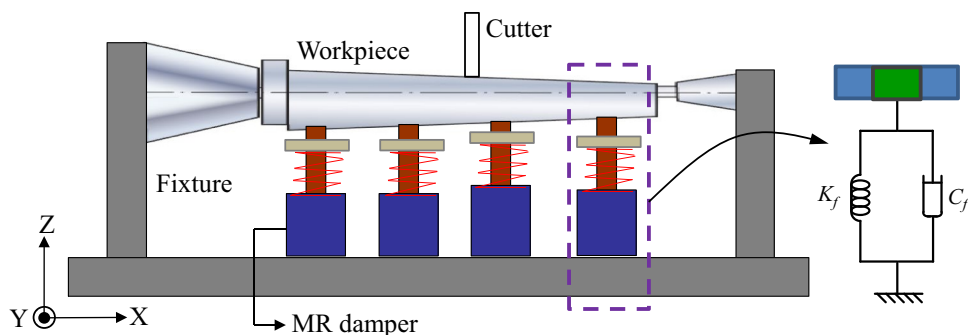
According to the above analysis, underdetermined fixture layout and initial cutting parameters, with materials removal, the dynamic damping and stiffness characteristics of the fixture-workpiece system can be reconstructed using MR dampers in milling of the thin-walled workpiece, which can improve the dynamic characteristics of machining system and keep the machining system stable for a long time.

3 Fixture-workpiece system dynamic characteristics reconstruction model

3.1 Dynamic characteristics reconstruction strategy

With the loss of generality, the dynamic milling force is viewed as an external load exerted on the fixture-workpiece system, then, the stable milling boundary is calculated and the stable milling parameters are selected. For obtaining the dynamic characteristics evolution process of MR damping fixture-workpiece system considering material removal, the

Fig. 1 Schematic diagram of MR damping fixture-workpiece system



dynamic cutting forces in the time domain given by Altintas [29] are used to calculate stability limit depth of cut and spindle speed, which can be used for expressing the damping and stiffness parameters explicitly for reconstructing the dynamic characteristics of the machining system. Therefore, the dynamic milling forces can be expressed as

$$\begin{bmatrix} F_x(t) \\ F_y(t) \\ F_z(t) \end{bmatrix} = \frac{N}{4\pi} a_p K_t A_0 \begin{bmatrix} \Delta x(t) \\ \Delta y(t) \\ \Delta z(t) \end{bmatrix} \tag{4}$$

where A_0 denotes time-varying directional dynamic milling force coefficients, which are determined by the Fourier series expansion method. a_p represents the depth of the cut. $\Delta x(t)$, $\Delta y(t)$, and $\Delta z(t)$ are the dynamic displacements of cutter in X -, Y -, and Z -directions.

In milling, significant interaction occurs between the cutter and the workpiece. Hence, considering the complexity of the frequency response function, the dynamic milling force Eq. (4) in the frequency domain can be given by

$$\begin{bmatrix} F_x(i\omega_c) \\ F_y(i\omega_c) \\ F_z(i\omega_c) \end{bmatrix} = \frac{N}{4\pi} a_p K_t (1 - e^{-i\omega_c T}) A_0 \mathbf{G} \begin{bmatrix} F_x(i\omega_c) \\ F_y(i\omega_c) \\ F_z(i\omega_c) \end{bmatrix} \tag{5}$$

where ω_c denotes the chatter frequency in milling. T is the cutter tooth passing period. \mathbf{G} represents the transfer function between tool and workpiece and can be defined as follows:

$$\mathbf{G} = \mathbf{G}_w + \mathbf{G}_c = \begin{bmatrix} G_{xx}(i\omega_c) & G_{xy}(i\omega_c) & G_{xz}(i\omega_c) \\ G_{yx}(i\omega_c) & G_{yy}(i\omega_c) & G_{yz}(i\omega_c) \\ G_{zx}(i\omega_c) & G_{zy}(i\omega_c) & G_{zz}(i\omega_c) \end{bmatrix} \tag{6}$$

For thin-walled workpieces, the cutter is regarded as rigidity compared to the workpiece. Considering the workpiece geometry and tool path in the milling of thin-walled parts, several experiments show that the vibration in Z -direction is the dominant mode compared with that in X - and Y -directions, which can be verified by Zhou et al. [30]. Hence, for simplification, the dynamic milling forces in X - and Y -directions can be ignored. Subsequently, the 3D chatter stability model described here can be simplified as a 1D model in the Z -direction. Then, the stability problem of Eq. (5) is reduced to the following:

$$F_z(i\omega_c) = \frac{N}{2\pi} a_p K_t \alpha_{zz} \text{Re}[\mathbf{G}_z(i\omega_c)] F_z(i\omega_c) \tag{7}$$

with

$$\alpha_{zz} = \phi \left[-K_r (\cos 2\kappa + 1) + K_a \sin 2\kappa \right] \Big|_{\phi_{st}}^{\phi_{ex}} \tag{8}$$

$$\text{Re}[\mathbf{G}_z(i\omega_c)] = \frac{1 - r^2}{k_z \left[(1 - r^2)^2 + (2\zeta r)^2 \right]} \tag{9}$$

where K_t , K_r , and K_a represent cutting force coefficients in tangential, radial, and axial directions, respectively. k_z is the normal stiffness of the workpiece. ζ denotes the damping ratio. $r = \omega_c / \omega_n$ and ω_n are the natural frequency.

Therefore, the stability limit depth of cut and the spindle speed are calculated as follows:

$$a_{\text{lim}} = \frac{2\pi}{NK_t \alpha_{zz} \text{Re}[\mathbf{G}_z(i\omega_c)]} \tag{10}$$

$$n = \frac{30\omega_c}{N \left[(k + 1)\pi - \arctan \left(\frac{r^2 - 1}{2\zeta r} \right) \right]} \tag{11}$$

From Eqs. (10) to (11), the limit depth of cut increases by means of regulating the damping and stiffness parameters of the machining system. Hence, the proposed method is used to reconstruct the dynamic characteristics using the MR dampers. For the fixture-workpiece system, underdetermined process parameters and fixture layout, with materials removal, the dynamic characteristics of the machining system decrease and the vibration enhances. Then, the output dynamic characteristics of MR dampers are regulated by current, which can offset the energy loss.

Subsequently, for the fixture-workpiece system, the dynamic characteristic reconstruction method of the system must satisfy the constraint of spindle speed n :

$$\begin{cases} 0 < n \leq n_{\text{max}} \\ n = \frac{60f}{N \cdot k} \quad (k = 1, 2, 3 \dots) \end{cases} \tag{12}$$

where f is tool passing frequency. n_{max} denotes the maximum allowable spindle speed of machine tool.

For the axial depth of cut a_p , it needs to meet the following constraints:

$$\begin{cases} 0 < a_p \leq a_{p\text{max}} \\ 0 < a_p \leq a_{p\text{lim}}(n) \end{cases} \tag{13}$$

where a_p is the initial selected axial cutting depth in the process. $a_{p\text{max}}$ denotes the maximum depth of cut. $a_{p\text{lim}}(n)$ represents the stable limit depth of cut, which needs to match with spindle speed n .

According to Eqs. (12) and (13), with material removal, to ensure that the optimal cutting parameters keep in a stable cutting area for a long time, the dynamic parameters of the fixture-workpiece system in each cutting state are calculated based on structural dynamic modification

method, then, the stability diagram lobes are plotted as shown in Fig. 2. Next, it can be determined whether the optimal cutting parameters are still in the absolute stable region. If it is in the absolute stable region, machining continues. Otherwise, the stability limit depth of cut $a_{p\text{lim}}^i$ in this state is calculated.

Considering the initial stable limit depth of cut $a_{p\text{lim}}$ before machining, the change of stable limit depth of cut $\Delta a_{p\text{lim}}$ before and after machining can be calculated. Therefore, the change of stable limit depth of cut $\Delta a_{p\text{lim}}$ can be determined by

$$\begin{cases} \Delta a_p = a_{p\text{lim}} - a_p \\ \Delta a_{p\text{lim}} = a_{p\text{lim}} - a_{p\text{lim}}^i \quad (i = 1, 2, 3 \dots) \end{cases} \quad (14)$$

where Δa_p is the allowance value of the initially selected depth of cut a_p corresponding to the initial limit depth of cut $a_{p\text{lim}}$, $a_{p\text{lim}}^i$ is the stable limit depth of cut under the i -th cutting state.

When $a_{p\text{lim}}^i$ is greater than a_p , the machining process is stable and continues. While $a_{p\text{lim}}^i$ is less than a_p , the machining process is unstable, and the dynamic characteristic of the machining system needs to adjust for further machining. Therefore, it can be seen from Fig. 2 that for obtaining better dynamic characteristic reconstruction effect of the fixture-workpiece system, the limit depth of cut $a_{p\text{lim}}^h$ of the reconstructed fixture-workpiece system must meet:

$$a_{p\text{lim}}^h \geq a_p + \Delta a_p \quad (15)$$

In short, according to the stability prediction model Eqs. (10), (11) and (15), the appropriated control currents i of MR dampers in the fixture-workpiece system are

calculated, which can be used to reconstruct the dynamic characteristics of the fixture-workpiece system by means of the stiffness and damping factor outputted by MR dampers, and enlarge the stable cutting region and improve machining stability.

3.2 Solution of the time-varying modal parameters and reconstructed currents in milling

From Eqs. (10) to (11), it can be found that modal parameters such as natural frequency, damping ratio, and stiffness are closely related to the milling system stability. Due to material removal and MR dampers, the modal parameters of the milling system are time-varying. Therefore, to reconstruct the dynamic characteristics of the fixture-workpiece system, the time-varying modal parameters should be identified accurately based on the structural dynamic modification method, and the modified process is shown in Fig. 3.

Then, introducing an auxiliary equation is

$$(M_{W,0} + \Delta M_{W,m})\ddot{q}_W(t) - (M_{W,0} + \Delta M_{W,m})\dot{q}_W(t) = \mathbf{0} \quad (16)$$

Combining Eqs. (3) and (16), and rearranging the resulting expressions in matrix form yields

$$(A_{W,0} + \Delta A_{W,m} + A_{i,m})\dot{x}_W(t) + (B_{W,0} + \Delta B_{W,m} + B_{i,m})x_W(t) = F_W(t) \quad (17)$$

where $A_{W,0} = \begin{bmatrix} C_{W,0} & M_{W,0} \\ M_{W,0} & \mathbf{0} \end{bmatrix}$, $\Delta A_{W,m} = \begin{bmatrix} \Delta C_{W,m} & \Delta M_{W,m} \\ \Delta M_{W,m} & \mathbf{0} \end{bmatrix}$,
 $A_{i,m} = \begin{bmatrix} C_{i,m} & \mathbf{0} \\ \mathbf{0} & \mathbf{0} \end{bmatrix}$, $B_{W,0} = \begin{bmatrix} K_{W,0} & \mathbf{0} \\ \mathbf{0} & -M_{W,0} \end{bmatrix}$, $\Delta B_{W,m} = \begin{bmatrix} \Delta K_{W,m} & \mathbf{0} \\ \mathbf{0} & -\Delta M_{W,m} \end{bmatrix}$, $B_{i,m} = \begin{bmatrix} K_{i,m} & \mathbf{0} \\ \mathbf{0} & \mathbf{0} \end{bmatrix}$, $x_W(t) = \begin{bmatrix} q_W(t) \\ \dot{q}_W(t) \end{bmatrix}$,

Fig. 2 Dynamic characteristic reconstruction strategy of MR damping fixture-workpiece system

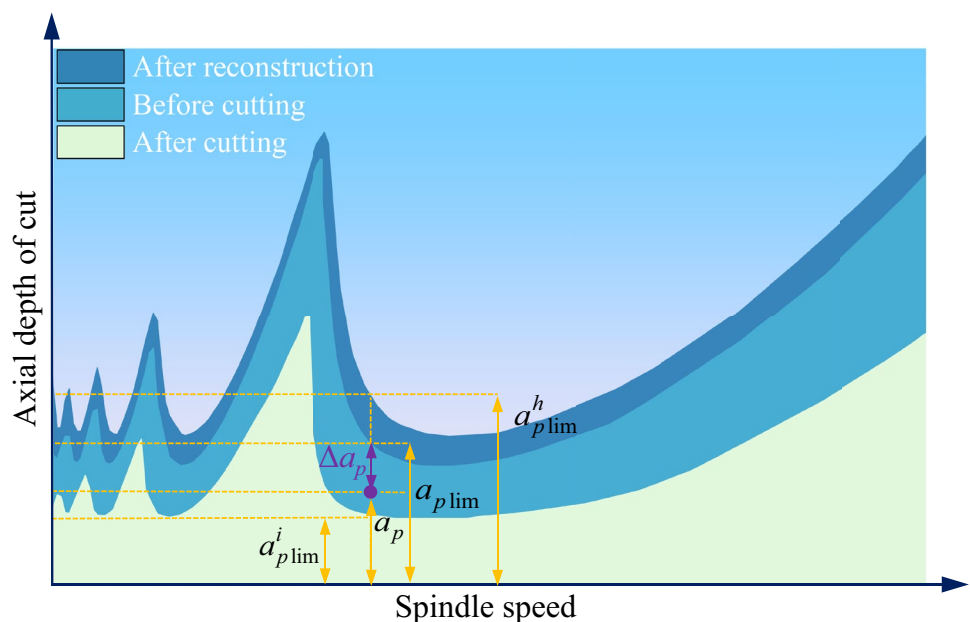
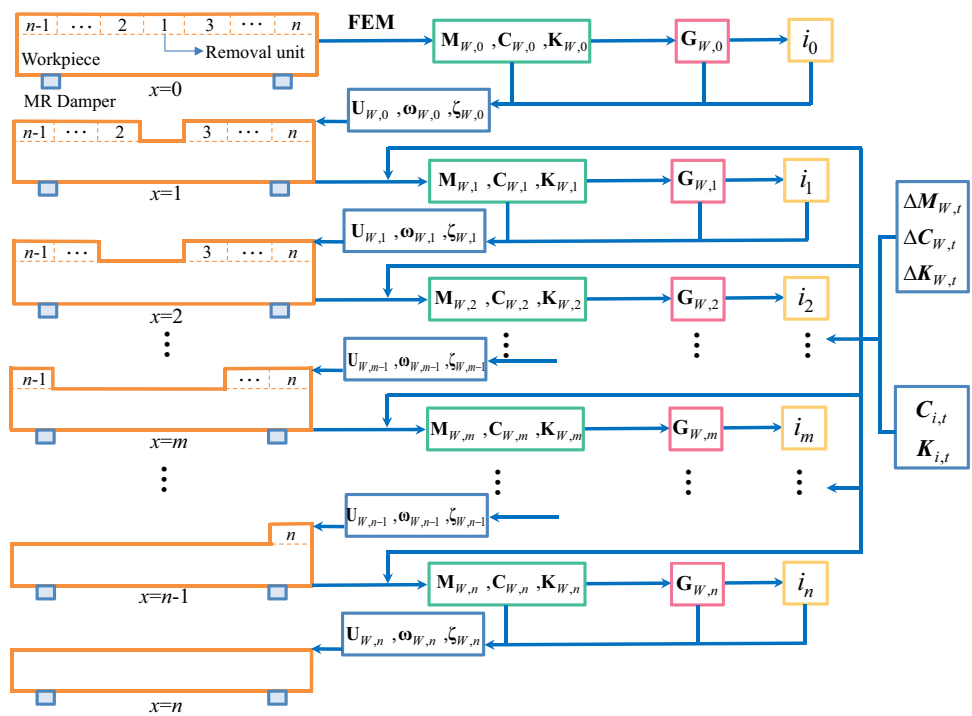


Fig. 3 Calculation procedure for the dynamics time-varying modal parameters



$\mathbf{F}_W(t) = \begin{bmatrix} \mathbf{F}_{z,m}(t) - P_{z,m}\mathbf{z} \\ \mathbf{0} \end{bmatrix}$. In addition, the subscript ‘ W ’ denotes the workpiece–fixture system, the subscript ‘ m ’ expresses the m -th workpiece state, and the subscript ‘ 0 ’

where Λ_0 and Λ_0^* are the conjugate complex eigenvalues, Ψ_0 and Ψ_0^* are the conjugate complex mode shape matrix.

Substituting Eq. (18) into (17) and premultiplying this equation by $\mathbf{U}_{W,0}^T$, we obtain

$$\mathbf{U}_{W,0}^T(\mathbf{A}_{W,0} + \Delta\mathbf{A}_{W,m} + \mathbf{A}_{i,m})\mathbf{U}_{W,0}\dot{\Gamma}_{W,0}(t) + \mathbf{U}_{W,0}^T(\mathbf{B}_{W,0} + \Delta\mathbf{B}_{W,m} + \mathbf{B}_{i,m})\mathbf{U}_{W,0}\Gamma_{W,0}(t) = \mathbf{U}_{W,0}^T\mathbf{F}_W(t) \tag{20}$$

expresses the initial state.

To better determine the modal parameters of the milling system under time-varying conditions, the equation of the milling system is transformed from a physical space coordinate system to a modal space coordinate system. Thus, by defining vector $\mathbf{x}_W(t)$ as

$$\mathbf{x}_W(t) = \mathbf{U}_{W,0}\Gamma_{W,0}(t) \tag{18}$$

In general, in complex modal coordinate system,

$$\begin{cases} \mathbf{U}_{W,0}^T\mathbf{A}_{W,0}\mathbf{U}_{W,0} = \text{diag}(\mathbf{a} \ \mathbf{a}^*) \\ \mathbf{U}_{W,0}^T\mathbf{B}_{W,0}\mathbf{U}_{W,0} = \text{diag}(\mathbf{b} \ \mathbf{b}^*) \end{cases} \tag{21}$$

where a and a^* , b , and b^* are conjugate complex numbers, respectively.

Therefore, Eq. (21) is reduced to

$$\begin{bmatrix} \text{diag}(\mathbf{a} \ \mathbf{a}^*) + \mathbf{U}_{W,0}^T\Delta\mathbf{A}_{W,m}\mathbf{U}_{W,0} + \mathbf{U}_{W,0}^T\mathbf{A}_{i,m}\mathbf{U}_{W,0} \end{bmatrix} \dot{\Gamma}_{W,0}(t) + \begin{bmatrix} \text{diag}(\mathbf{b} \ \mathbf{b}^*) + \mathbf{U}_{W,0}^T\Delta\mathbf{B}_{W,m}\mathbf{U}_{W,0} + \mathbf{U}_{W,0}^T\mathbf{B}_{i,m}\mathbf{U}_{W,0} \end{bmatrix} \Gamma_{W,0}(t) = \mathbf{U}_{W,0}^T\mathbf{F}_{W,m}(t) \tag{22}$$

where $\Gamma_{W,0}(t)$ represents the initial modal displacement vector of the workpiece. $\mathbf{U}_{W,0}$ denotes the initial modal shape matrix of the workpiece and can be expressed as

$$\mathbf{U}_{W,0} = \begin{bmatrix} \Psi_0 & \Psi_0^* \\ \Psi_0\Lambda_0 & \Psi_0^*\Lambda_0^* \end{bmatrix} \tag{19}$$

For the milling of the thin-walled workpiece, the modal parameters such as mass, stiffness, and damping in different machining states are difficult to obtain accurately. Therefore, assuming that the mass, stiffness, and damping are monotonic decreasing functions in milling, and the change of the parameters is the same value in each cutting step, we obtain

$$\begin{cases} \Delta \mathbf{A}_{W,m} = \frac{(\mathbf{A}_n - \mathbf{A}_0)m}{l} \\ \Delta \mathbf{B}_{W,m} = \frac{(\mathbf{B}_n - \mathbf{B}_0)m}{l} \end{cases} \quad (23)$$

where l is the length of the cutting path, \mathbf{A}_0 and \mathbf{B}_0 represent initial system information, and \mathbf{A}_n and \mathbf{B}_n denote system information after milling.

Thus, the characteristic equation $\mathbf{G}_{W,m}$ of Eq. (23) can be given by

$$\left\{ \lambda \left[\text{diag}(\mathbf{a} \mathbf{a}^*) + \mathbf{U}_{W,0}^T \Delta \mathbf{A}_{W,m} \mathbf{U}_{W,0} + \mathbf{U}_{W,0}^T \mathbf{A}_{i,m} \mathbf{U}_{W,0} \right] + \left[\text{diag}(\mathbf{b} \mathbf{b}^*) + \mathbf{U}_{W,0}^T \Delta \mathbf{B}_{W,m} \mathbf{U}_{W,0} + \mathbf{U}_{W,0}^T \mathbf{B}_{i,m} \mathbf{U}_{W,0} \right] \right\} \begin{bmatrix} \boldsymbol{\Psi} \\ \boldsymbol{\Psi} \lambda \end{bmatrix} = \mathbf{0} \quad (24)$$

For $\mathbf{A}_{i,m}$ and $\mathbf{B}_{i,m}$ caused by MR dampers, the modified Bouc–Wen model is adopted to describe the dynamic characteristics of the MR dampers, and the damping force can be written as

$$\mathbf{F}_{B-W} = \mathbf{C}_i \dot{\mathbf{q}} + \mathbf{K}_i \mathbf{q} + \mathbf{P}_i \mathbf{z} \quad (25)$$

where the model parameters \mathbf{C}_i , \mathbf{K}_i , and \mathbf{P}_i are related to control current i of MR dampers, and based on the measured data of MR damper, the cubic polynomial is used to express the element of model parameters of the dampers, and

$$\begin{cases} C_{i,m}(i) = \alpha_1 i^3 + \alpha_2 i^2 + \alpha_3 i + \alpha_4 \\ K_{i,m}(i) = \beta_1 i^3 + \beta_2 i^2 + \beta_3 i + \beta_4 \\ P_{i,m}(i) = \gamma_1 i^3 + \gamma_2 i^2 + \gamma_3 i + \gamma_4 \end{cases} \quad (26)$$

where $\alpha_1, \alpha_2, \alpha_3, \alpha_4, \beta_1, \beta_2, \beta_3, \beta_4, \gamma_1, \gamma_2, \gamma_3,$ and γ_4 are calibrated by the measured force and displacement data of MR dampers.

Substituting Eqs. (25) and (26) into Eq. (24), the complex eigenvalues and complex eigenvectors of Eq. (24) can be calculated and given by

$$\boldsymbol{\Lambda}'_{W,m} = \text{diag}(\boldsymbol{\Lambda} \boldsymbol{\Lambda}^*) = \text{diag}(\lambda_1 \lambda_2 \cdots \lambda_n \lambda_1^* \lambda_2^* \cdots \lambda_n^*) \quad (27)$$

$$\boldsymbol{\Phi}_{W,m} = \begin{bmatrix} \boldsymbol{\Psi}_m & \boldsymbol{\Psi}_m^* \\ \boldsymbol{\Psi}_m \boldsymbol{\Lambda}_m & \boldsymbol{\Psi}_m^* \boldsymbol{\Lambda}_m^* \end{bmatrix} \quad (28)$$

Subsequently, it is found that from Eq. (24), the relationship of modal displacement at the present moment and that at the previous moment, which can be given by

$$\boldsymbol{\Gamma}_{W,0} = \boldsymbol{\Phi}_{W,m} \boldsymbol{\Gamma}_{W,m} \quad (29)$$

Substituting Eq. (29) into Eq. (18), we obtain the relationship between present physical space coordinates and modal coordinates

$$\mathbf{x}_W(t) = \mathbf{U}_{W,m} \boldsymbol{\Gamma}_{W,m}(t) \quad (30)$$

where $\mathbf{U}_{W,m}$ denotes the modal shape matrix at the present moment, which can be expressed as

$$\mathbf{U}_{W,m} = \mathbf{U}_{W,0} \boldsymbol{\Phi}_{W,m} \quad (31)$$

Therefore, according to Eq. (24), the natural frequencies, damping ratio, and stiffness of the dynamic milling system in

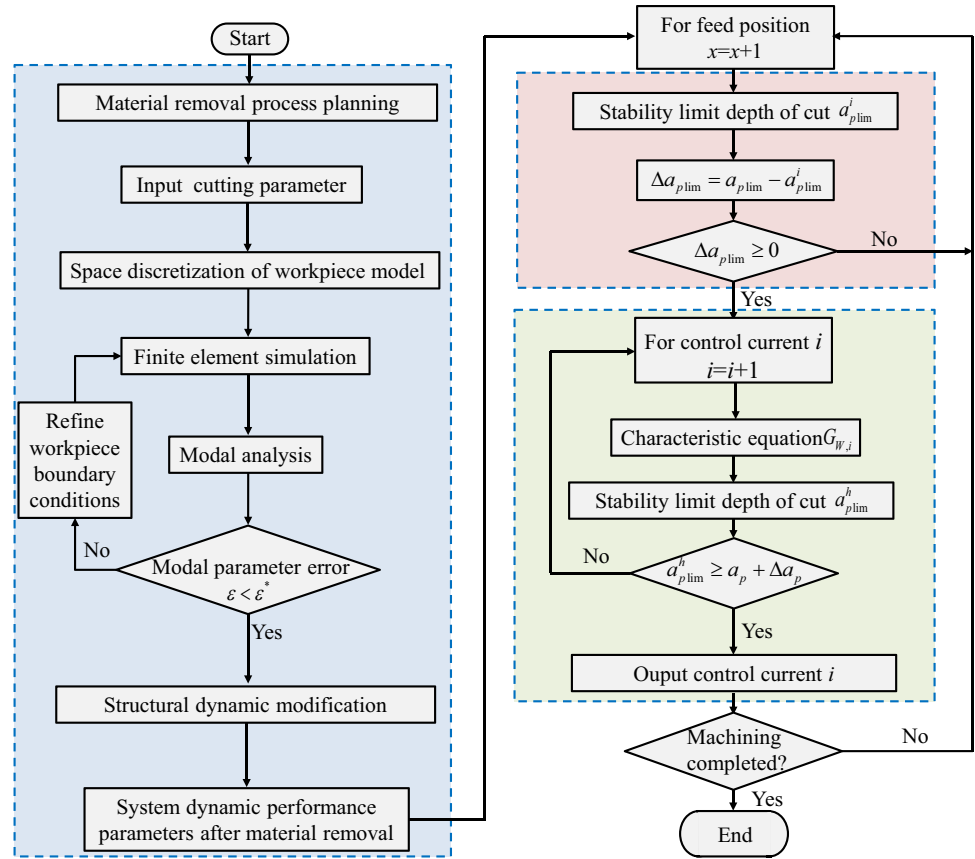
the m -th machining states can be obtained by

$$\begin{cases} \omega_{W,m,n} = \sqrt{\text{Re}^2(\lambda_n) + \text{Im}^2(\lambda_n)} \\ \zeta_{W,m,n} = \frac{\text{Re}(\lambda_n)}{\omega_{W,m,n}} \\ K_{W,m,n} = [\text{Re}^2(\lambda_n) + \text{Im}^2(\lambda_n)] \boldsymbol{\Psi}_m^T [\mathbf{M}_{W,0} + \Delta \mathbf{M}_{W,m}] \boldsymbol{\Psi}_m^* \end{cases} \quad (32)$$

Similarly, based on the parameters given in Eq. (32), the modal parameters at any moment in the milling of a thin-walled workpiece can be obtained.

Next, from the above analysis and calculation, the dynamic characteristics reconstructed scheme can be determined. At first, before machining, the material removal process should be planned, and the input cutting parameters are selected. Then, the thin-walled workpiece model is discretized in space, and the modal parameters are obtained by finite element method and modified by experimental modal analysis, so the accurate modal parameters that meet the machining requirements are obtained. Subsequently, the initial axial limit depth of cut a_{plim} can be obtained from Eq. (10). In addition, when material removal increases with machining, the system modal parameters (the natural frequencies $\omega'_{W,m}$, damping ratio $\zeta'_{W,m}$, and stiffness $K'_{W,m}$) of different machining conditions can be calculated by the method of structural dynamic modification according to Eqs. (16), (17), (18), (19), (20), (21), (22), (23), (24), (25), (26), (27), (28), (29), (30), (31) and (32), and the stability diagrams in every machining stage can be determined. Based on this, the stability of the machining stage is judged by Eqs. (10), (11), (12), (13), (14) and (15), namely, in constant spindle speed, whether the axial limit cutting depth is within the absolute stability region or not. If the axial limit cutting depth is in the stable area, the machining continues. Otherwise, the dynamic damping and stiffness of the fixture-workpiece system should be improved by adjusting MR dampers. To obtain the required current of system

Fig. 4 Flowchart of dynamic characteristic reconstruction current of MR damping fixture-workpiece system

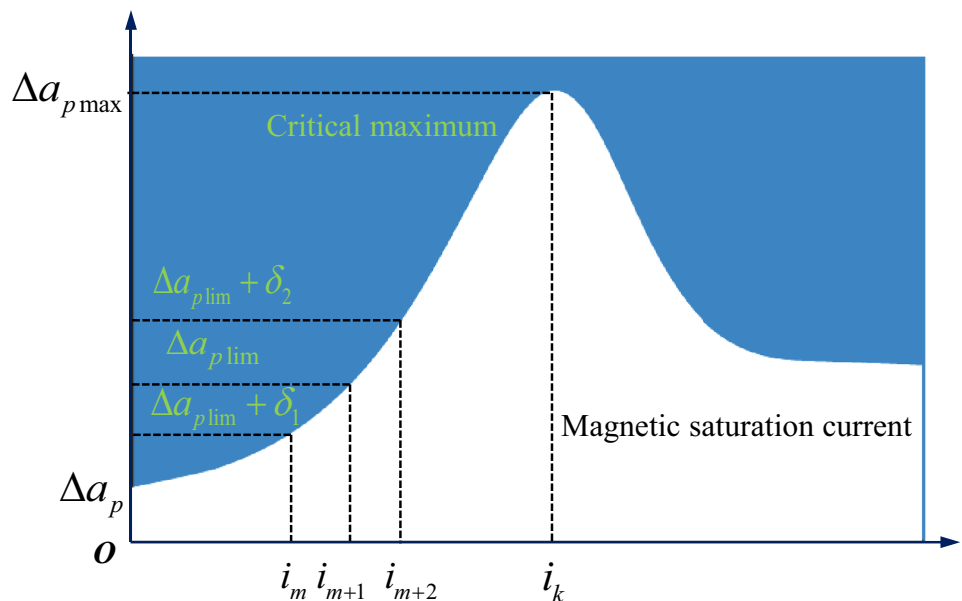


dynamic characteristics reconstruction for stable machining, the above calculation process is iterative until the requirements are met, and the calculated process of system dynamic characteristic reconstruction current is illustrated in Fig. 4.

During the iteration process, considering the dynamic characteristics of the MR dampers and the saturation

magnetization of MR fluids, optimal selection range of control current parameters for MR damping fixture is $[0, i_k]$, and calculation accuracy $|i_{m+1} - i_m| \leq 10^{-4}$, $m, m + 1 \in [0, i_k]$. Dynamic characteristics reconstruction scheme satisfied the stable machining is determined. After continuous calculation, control currents of MR damping

Fig. 5 Relationship between control current and the limit depth of cut in MR damping control system



fixture-workpiece system are obtained and shown in Fig. 5. From Fig. 5, with the increase of current, the growth of the limit depth of cut $\Delta a_{p\text{lim}}(i)$ is. However, when the control currents increase to i_k , the maximum limit depth of cut is decreased gradually. The reason for this is that the magnetic field intensity exceeds the maximum value, so the performance of MR fluids reduces, which causes the depth of cut to decrease. From here, we see that under the magnetic saturation, the damping and stiffness properties of the fixture-workpiece system can be improved using MR dampers with material removal, and the machining is stable for a long time.

4 Experimental verification and discussion

A series of experiments using four MR dampers are conducted to verify the effectiveness of the proposed method in the milling of the thin-walled plate. A novel MR damper is designed and used to establish a MR damping fixture to provide extra damping and stiffness characteristics for the thin-walled plate. Then, the modal parameters of the MR fixture-workpiece system can be obtained by impact experiments, which are applied to calculate the limit depth of cut in different conditions. Finally, many machining experiments are conducted on the three-axis milling center (YHVT8507) to validate the effect of MR dampers on the fixture-workpiece system.

4.1 Dynamic properties of MR damper

Squeezed MR damper contains MR fluids, supporting rod, upper and down cover, extruded plate, magnetic separator ring, excitation coil, shell, reset device, etc., whose properties of structures are closely associated with that MR damper. Therefore, in design, electrical pure iron with high magnetic permeability is applied to manufacture upper and down covers, extruded plates, and shells. In addition, MR fluids are prepared in the lab, the supporting rod is made of aluminum, and excitation coil is wound with copper wire, magnetic separator ring is copper. The overall size of the MR damper is diameter 70 mm, height 38 mm, and the MR damper and measuring devices are shown in Fig. 6.

For the MR damper in the fixture, its dynamic characteristics are measured, and the measuring devices are shown in Fig. 6a, b. In-low frequency vibration, the damping forces are measured under the amplitudes (0.01 mm, 0.05 mm, 0.1 mm, 0.2 mm, 0.3 mm, and 0.5 mm), frequency (1 Hz, 2 Hz, 3 Hz, 5 Hz, 6 Hz, and 10 Hz) and current (0 A, 0.25 A, 0.5 A, 1 A, 1.5 A, and 2 A) using Instron 8871 material testing machine. Then, under frequencies 2 Hz and 3 Hz, the relationships of vibration amplitude

and damping force under vibration amplitude 0.2 mm are shown in Fig. 6c, d. For high-frequency vibration, the device contains a steady-state exciter (JZK-2), power amplifier (YE1311E), dynamometer (Kistler 9255B), an acceleration sensor (Dytran3325F1-16,845), data acquisition system (DEWESoft-SIRIUS *i*), etc. Then, the force and displacement signals are obtained under different exciting frequencies (500 Hz, 600 Hz, 800 Hz, 900 Hz, 1000 Hz, etc.) and exciting currents (0 A, 0.5 A, 1 A, 1.5 A, 2 A, etc.). Subsequently, the force–displacement hysteresis curve of the MR damper in different currents under excited frequency 1000 Hz and the force–displacement hysteresis curve of the MR damper in different exciting frequencies under excited currents 2A are as shown in Fig. 6e, f. Finally, based on Eqs. (25) and (26), the model parameters can be calibrated by genetic algorithm using the measured data, and $\alpha_1 = 0.3324$, $\alpha_2 = -0.9768$, $\alpha_3 = 1.6430$, $\alpha_4 = 0.5883$, $\beta_1 = -0.1029$, $\beta_2 = 0.0764$, $\beta_3 = 1.047$, $\beta_4 = 2.1050$, $\gamma_1 = 0.1831$, $\gamma_2 = -0.7090$, $\gamma_3 = 1.2630$, and $\gamma_4 = 0.0197$.

4.2 Impact tests

An impact experiment is carried out in this section for obtaining the modal parameters of the MR damping fixture-workpiece system. In experiments, the dimension of the thin-walled plate made from stainless steel is 300×100 mm with a thickness of 3 mm, Young's modulus of the material is 195 GPa, the Poisson's ratio is 0.25, and the density of the material is 7930 kg/m^3 . The impact test system contains a model hammer (Kistler, 500 N), acceleration sensors (Dytran3325F1-16,847 and ref. sensitivity 10.25 mV/g .), SIRIUS ACC data acquisition instrument (DEWESoft-SIRIUS *i* series), and computer.

In order to validate the effectiveness of the MR damping fixture for dynamic characteristics reconstruction, the impact tests and machining setup are shown in Fig. 7a. It is well known that different impact points on the thin-walled plate can generate different responses. Considering the four MR dampers constraints, the two edges of the thin-walled plate along the long direction are fixed on the fixture, and four MR dampers are located in the fixture, which can provide support force for thin-walled plate, and the impact measured points 1, 2, and 3 are distributed on the thin-walled plate as shown in Fig. 7b. We found that point 1 and point 3 are symmetric with respect to point 2, while point 2 is located in the middle of the thin-walled plate. Subsequently, all the vibration responses are obtained and analyzed in different measured points. Experimental results are shown that the vibration responses at point 1 are equal to that at point 3 due to the measured point symmetry on the plate. Then, the frequency response functions on points 1, 2, and 3 are obtained and shown in Fig. 8a. From Fig. 8a, we found that

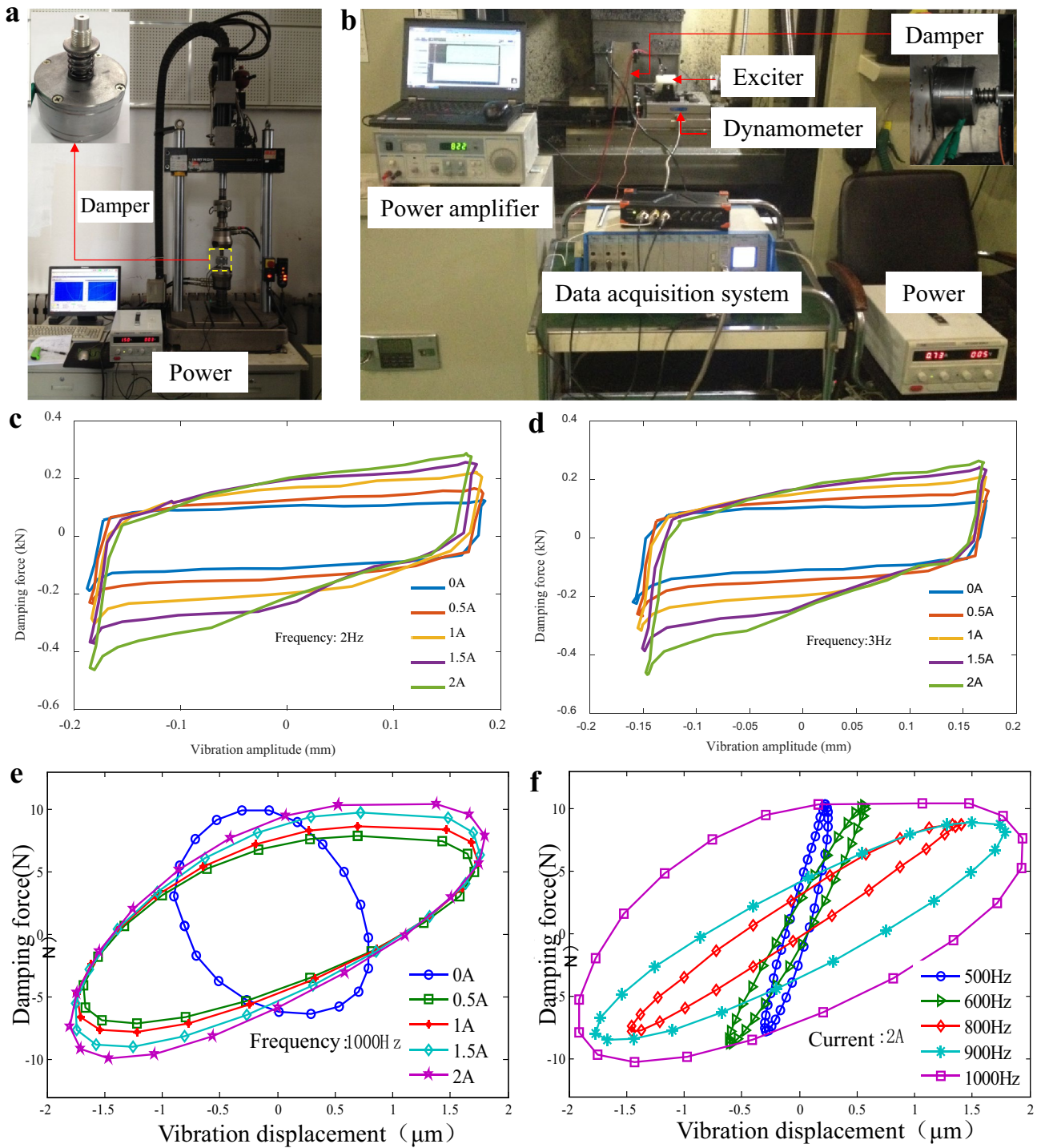


Fig. 6 Dynamic characteristics of MR damper under different conditions. **a** Low frequency vibration test devices; **b** High frequency vibration test devices; **c** and **d** relationship of vibration amplitude

and damping force under different current, amplitude, and frequency; **e** and **f** force–displacement hysteresis curve of MR damper under excited current and frequency

the natural frequencies on points 1, 2, and 3 are equal, but the amplitude on point 2 is smaller and more stable than that on points 1 and 3, therefore, the representative stable point 2 are selected for measuring responses, which is

shown in Fig. 7c. Then, the frequency response functions (FRFs) before and after MR damping activation under different currents are described in Fig. 8b, and the identified modal parameters are calculated and listed in Table 1. From

Fig. 7 Setups in impact tests/ machining and measured points 1, 2, and 3 on the thin-walled plate for impact tests

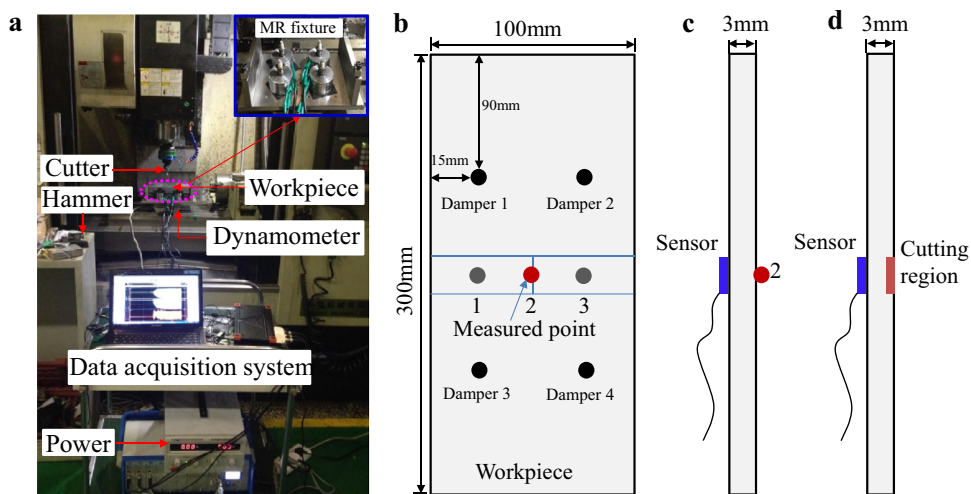


Fig. 8 Frequency response functions (FRFs) under different conditions. **a** Frequency response functions on points 1, 2, and 3; **b** frequency response functions before and after MR damping activation

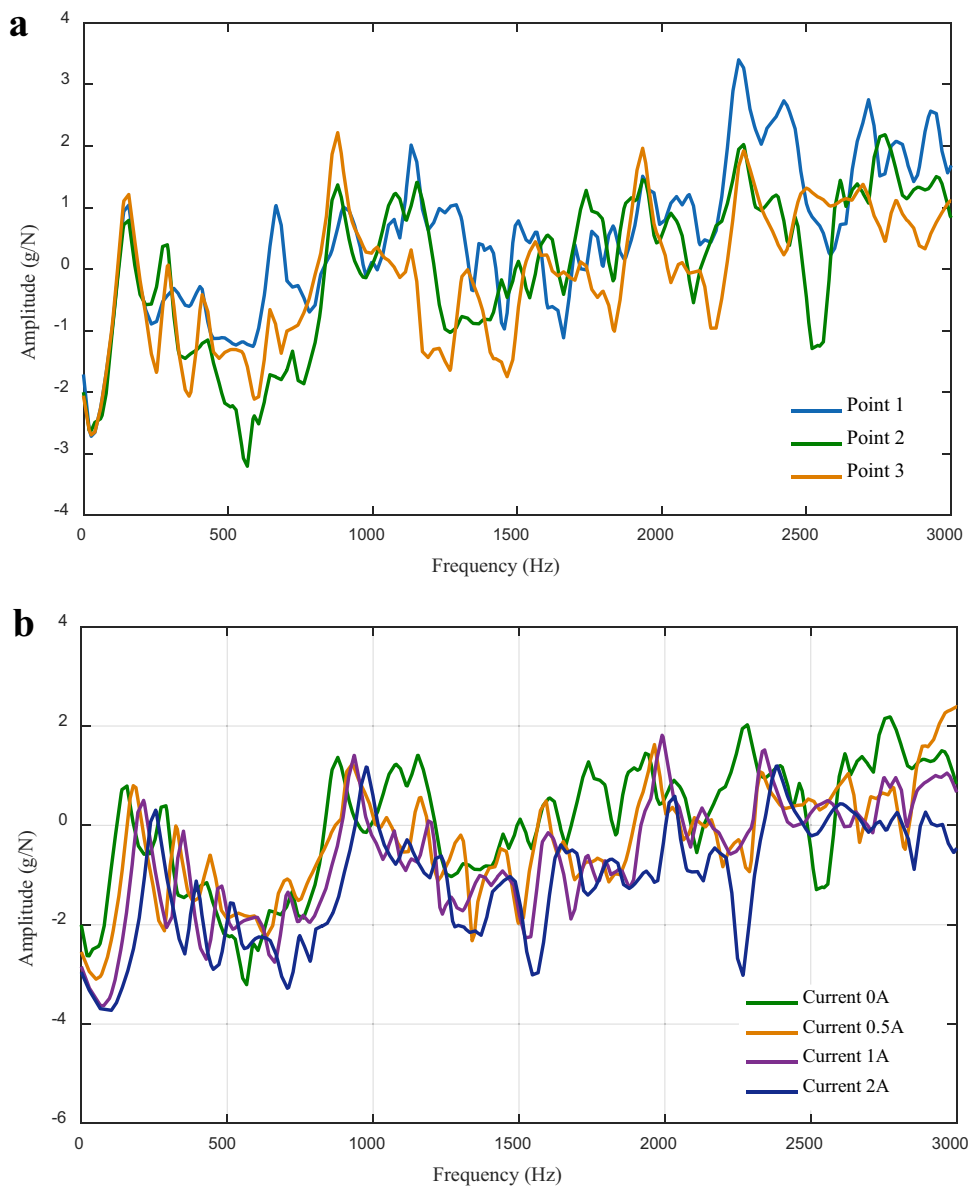


Table 1 Test system modal parameters

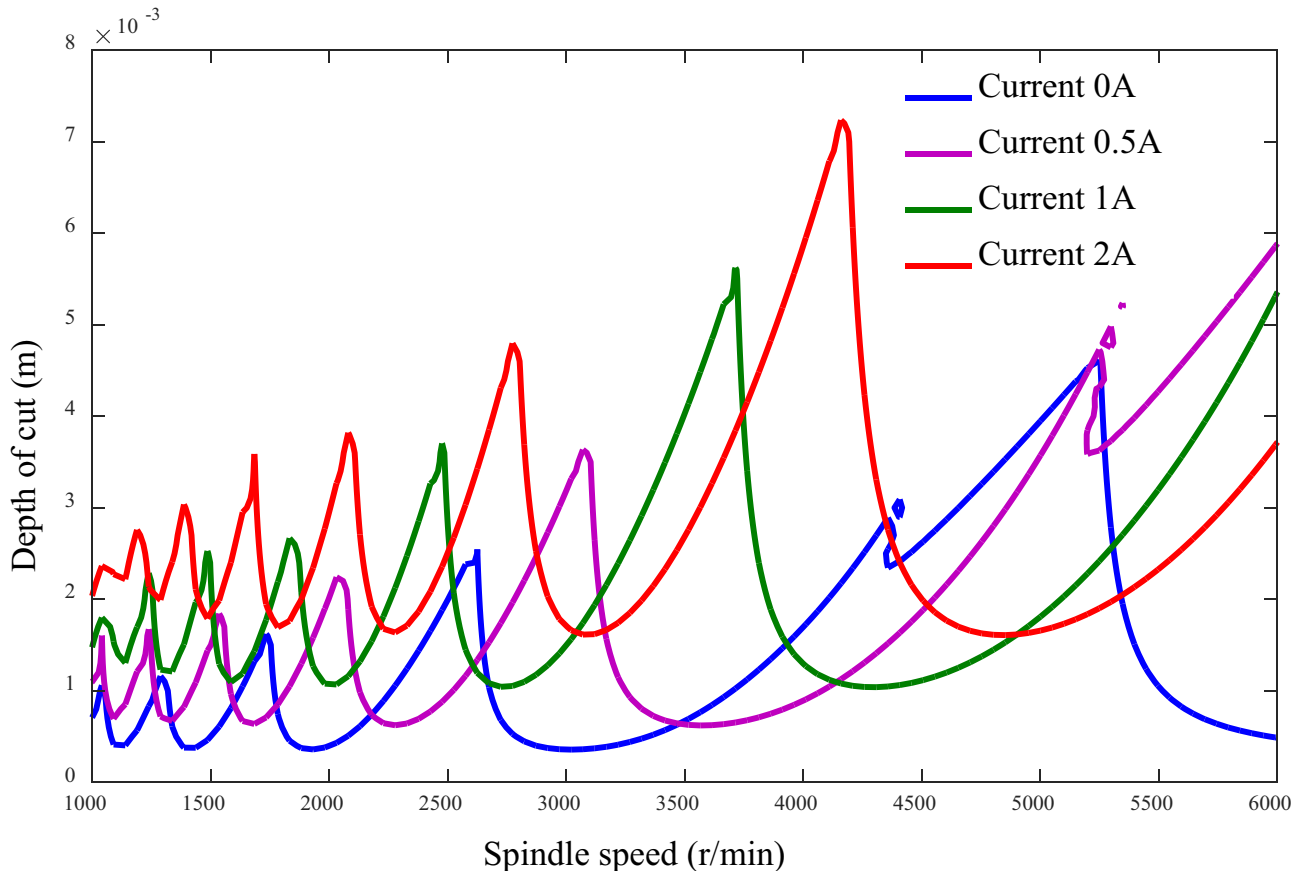
Current (A)	Natural frequency ω (Hz) (first order)	Damping ratio ζ	Normal stiffness k ($\text{N}\cdot\text{m}^{-1}$)
0	168.86	0.025	7.2848×10^4
0.5	197.60	0.032	7.8793×10^4
1	225.78	0.0368	1.4079×10^5
2	269.68	0.0443	2.7471×10^5

Fig. 8b and Table 1, we can see the dynamic properties of the workpiece-fixture system can be adjusted by MR dampers, the natural frequency, damping ratio, and normal stiffness are improved with the increasing of currents, which is the reason for designing a MR damping fixture in milling of the thin-walled workpiece.

To investigate the effect of MR dampers on the dynamic characteristics of the fixture-workpiece system, cutting force coefficients should be calibrated. Slot milling was conducted, and the machining parameters are spindle speed 2000 r/min, axial depth of cut 0.3 mm, feed rate 120 mm/min, 240 mm/min, 360 mm/min, 480 mm/min, and 600 mm/

min. The cutter used was a two-flute end milling cutter with a diameter of 12 mm and a helix angle of 30° . Then, based on Altintas [29], the cutting coefficients are calibrated as $K_{tc} = 207.5 \text{ N/mm}^2$, $K_{rc} = 2080 \text{ N/mm}^2$, $K_{ac} = 390.7 \text{ N/mm}^2$, $K_{te} = 63.69 \text{ N/mm}$, $K_{re} = 47.6 \text{ N/mm}$, and $K_{ae} = 20.397 \text{ N/mm}$. In addition, based on the test system modal parameters in Table 1, when no material removal is, stability diagram lobes in different control currents of the MR damping fixture for the machining system are shown in Fig. 9.

From Table 1 and Fig. 9, it is obviously seen that in different control currents of 0 A, 0.5 A, 1 A, and 2 A, the stability diagram lobes with on material removal are markedly different. With the increase of control current of the MR damping fixture-workpiece system, the natural frequency of the MR damping fixture-workpiece system increases significantly from 168.86 to 269.68 Hz, and the damping factor and the normal stiffness of the thin-walled workpiece improve simultaneously. More importantly, the stability diagram lobes move up and right directions in different currents of 0 A, 0.5 A, 1 A, and 2 A, and the stable regions enlarge greatly. Therefore, it can be seen that the damping and stiffness characteristics of the fixture-workpiece system can be changed by the MR dampers. Therefore, the feasibility of

**Fig. 9** Stability diagram lobes for the MR damping fixture-workpiece system with parameters in Table 1

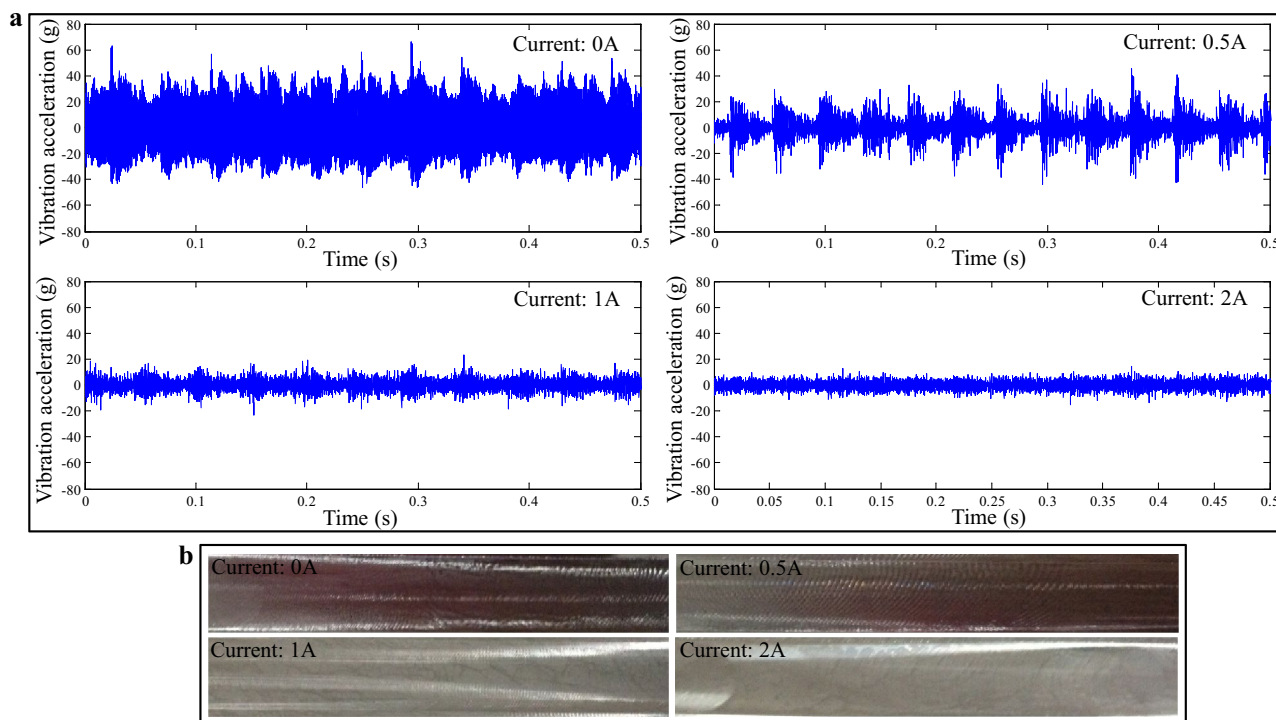


Fig. 10 Acceleration responses and machining surface of the fixture-workpiece system in different control currents. **a** Vibration acceleration responses of thin-walled workpiece in milling; **b** machining surface of thin-walled workpiece under different control currents

MR dampers in reconstructing the dynamic characteristics of the milling system is validated in modifying the dynamic characteristics of the fixture-workpiece system.

4.3 Effects of MR dampers on the MR fixture-workpiece system in milling

In order to investigate the effect of MR dampers on vibration suppression in the milling of the thin-walled workpiece, several milling tests are carried out. According to the stability diagram lobes of the fixture-workpiece system at different currents, as shown in Fig. 9, in milling of the thin-walled plate, several experiments at spindle speed 1000 r/min, 1500 r/min, 2000 r/min, 3000 r/min, and 6000 r/min and axial depth of cut 0.2 mm, 0.5 mm, 0.8 mm, and 1 mm are conducted, and four sample plates are used for experiments under currents of 0 A, 0.5 A, 1 A, and 2 A. While the machining region is shown in Fig. 7d, and the acceleration sensor is arranged in the middle of the workpiece face relative to the machining region. Then, the acceleration response of the milling system and the surface state at spindle speed 2000 r/min, feed speed 320 mm/min, and axial depth of cut 0.5 mm are obtained in different currents of 0 A, 0.5 A, 1 A, and 2 A, which are shown in Fig. 10.

From Fig. 10, when no control current is applied to the MR damping fixture-workpiece system, the vibration

acceleration signal fluctuates violently, the maximum amplitude of vibration acceleration is 60 g, and the machined surface is rough and has obvious vibration marks, which shows that chatter occurs. When the control current 0.5 A is exerted on the machining system, the amplitude of vibration acceleration response reduces obviously to 40 g, but the fluctuation state is sharp, and the machined surface quality has improved, but chatter also occurs. While the control currents of 1 and 2 A are exerted on the machining system, the value of vibration acceleration response is very low, the maximum acceleration value is less than 20 g, and the signal status is stable, the machined surface is smooth without vibration marks. Experimental results can further validate that the stability of the milling system can be effectively improved by reasonably adjusting the dynamic characteristics of the fixture-workpiece system with MR dampers.

4.4 Validation of the proposed method considering the effect of MR dampers

In order to verify the effectiveness of the proposed method, the same material and size of the thin-walled plate as the previous experiments are used. Row material removal form in the middle of the plates is selected, as shown in Fig. 11a. L1 is the initial state of the workpiece, L2 denotes the first cut, and L3 and L4 represent the second and third cut. Based on

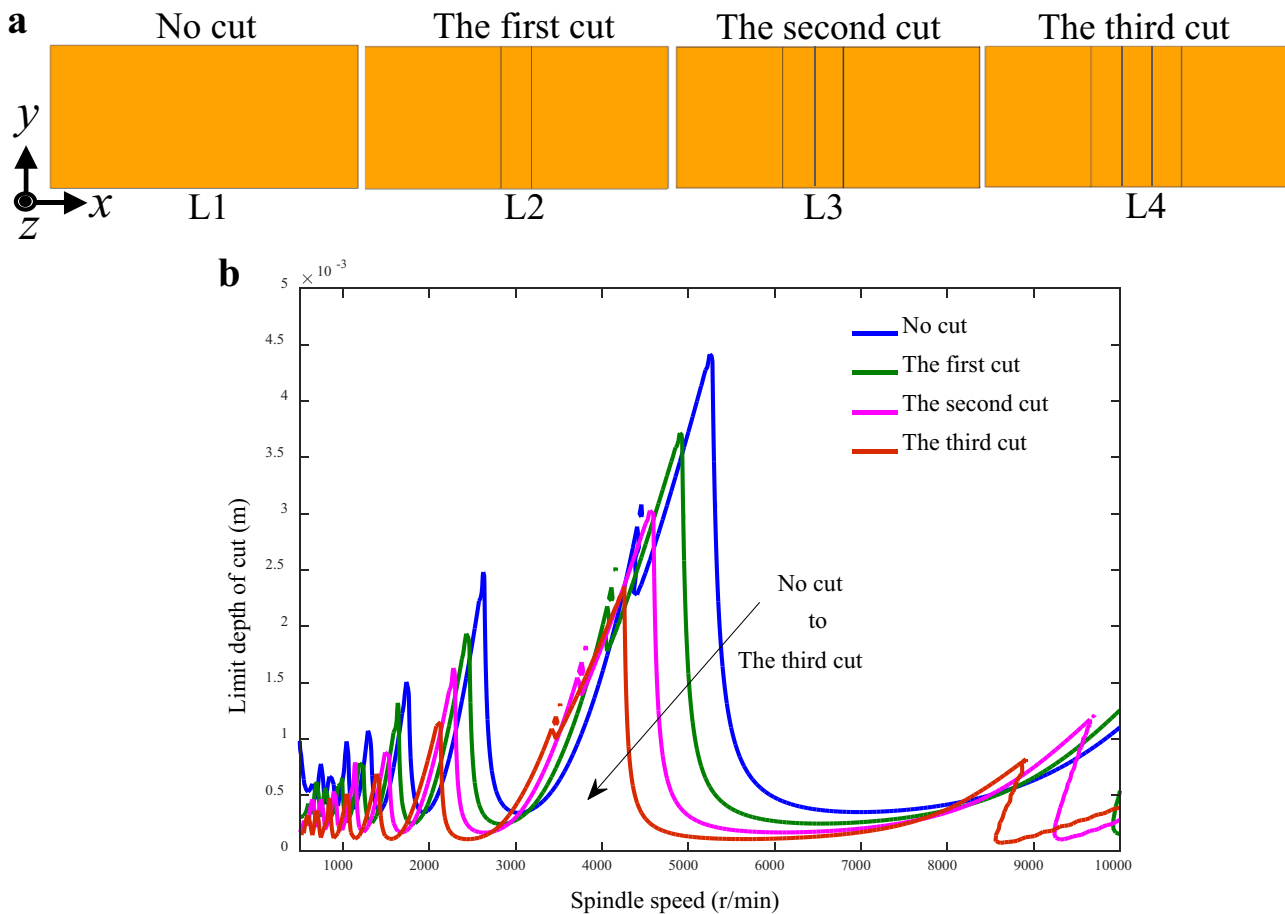


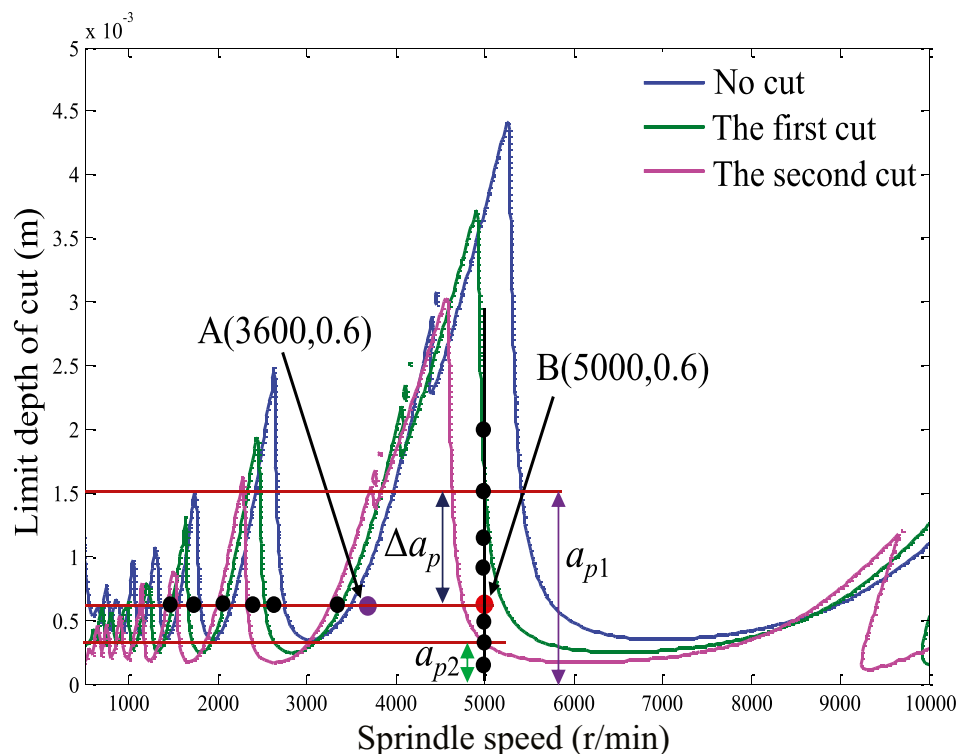
Fig. 11 Dynamic characteristics evolution process of machining system under different conditions. **a** Material removal form; **b** evolutionary process of system stability diagram lobes under row material removal form

Siemens NX and the experimental modal analysis method, the modal responses of the workpiece are obtained and analyzed, and the first-order natural frequency and corresponding stiffness are obtained in different material removal states. Subsequently, under different material removal states, the changes in stability diagram lobes are shown in Fig. 11b. From Fig. 11b, it can be seen that the row material removal method removes a large amount of material, the dynamic parameters of the machining system vary greatly, the system stability is obviously affected, and the stable limit cutting depth is reduced.

In order to overcome the disadvantage of vibration suppression only relying on cutting parameter optimization, a novel fixture using MR dampers is designed to reconstruct the dynamic characteristics of the machining system to keep a stable cutting state for a long time. For the row material removal form, the stability diagram lobes under no material removal, the first cut, and the second cut are shown in Fig. 12. Then, several machining experiments at spindle

speed of 1500 r/min, 1800 r/min, 2000 r/min, 2400 r/min, 2600 r/min, 3200 r/min, and 3600 r/min under the same depth of cut 0.6 mm, and at the depth of cut of 0.2 mm, 0.3 mm, 0.5 mm, 0.6 mm, 1.0 mm, 1.2 mm, 1.5 mm, and 2.0 mm under the same spindle speed 5000 r/min are carried out to analyze the machining system dynamic properties. In addition, the cutting parameters in point A (spindle speed 3600 r/min and axial depth of cut 0.6 mm) and point B (spindle speed of 5000 r/min and axial depth of cut of 0.6 mm) are marked in Fig. 12. From Fig. 12, we can see that point A is located in stable region. With material removal, the stability boundary moves to left, but the cutting parameter in point A is always in the absolute stable region until exceeding the right boundary. Compared with the cutting parameters at point A, the cutting parameters at point B is relatively conservative. When there is no material removal, it is located in the absolute stability region, while after the first cut, the stability boundary reduces but the machining system is still stable. However, after the second cut, the point B is

Fig. 12 Cutting parameters in point **A** and **B** under the row material removal form. The blue line is no cut, the green line denotes the first cut, and the purple line represents the second cut



located in unstable region. In this case, to ensure machining efficiency and do not change the initial fixture layout, the dynamic characteristics of machining system should be improved to guarantee the stable machining process. Therefore, to obtain the stable machining state, MR damping support fixture is designed and the dynamic characteristics reconstruction algorithm of the fixture-workpiece system is proposed in the paper.

Based on the reconstruction algorithm proposed in Sects. 2 and 3, from Fig. 12, in point B (spindle speed of 5000 r/min, axial depth of cut 0.6 mm), the depth of cut corresponding to the first cut and the second cut are $a_{p1} = 1.5$ mm and $a_{p2} = 0.35$ mm, so the change of depth of cut is $\Delta a_p = a_{p1} - a_{p2} = 1.15$ mm. According to Eqs. (10) and (16)–(32), the control current i of the MR damping fixture-workpiece system is calculated and $i = 0.7953$ A. Considering the limitation of the DC-regulated power supply, the control current $i = 1$ A is selected approximately. Subsequently, under control current of 1 A, the damping ratio and stiffness value of MR damping support fixture-workpiece system are calculated, and the damping ratio is 0.0363, stiffness value 1.635×10^4 N/m. Then, the stability diagram lobe reconstructed is shown in Fig. 13. It can be seen that point B is still located in a stable region, and the stable region is enlarged by adjusting the properties of MR dampers, which can keep the machining system stable for a long time.

In order to directly verify the effectiveness of the proposed reconstruction algorithm, the selected cutting parameters (spindle speed of 5000 r/min and axial depth of cut of 0.6 mm) are chosen. Under no control current and 1 A control current, the milling of the thin-walled plate is conducted. Then, the normal forces in Z-direction and the machined surface are obtained, and the cutting force signal is transformed by a fast Fourier transform. The experimental results are shown in Fig. 14. It can be seen from Fig. 14 that when no control current is exerted on the machining system, the dynamic cutting forces fluctuate greatly and the amplitude of it is between ± 200 N. In addition, from the cutting force spectrum, integral multiple of tool passing frequencies (167.4 Hz, 500.2 Hz, etc.) appear, and the chatter frequencies (654.7 Hz, 738.4 Hz, etc.) are also found, which indicates that chatter occurs during milling, and the spiral marks on the machined surface also prove that chatter occurs in machining. When the control current of 1 A is exerted on the machining system, the cutting force signal is stable, and the amplitude of the cutting force is much lower than that without current control. In the cutting force spectrum, only the integral multiple of tool passing frequency (167.4 Hz, etc.) appears, the amplitude is very small, and the machined surface is smooth, which can be shown that the dynamic characteristics of the fixture-workpiece system are improved by regulating the MR dampers in the fixture, and the machining chatter is suppressed effectively.

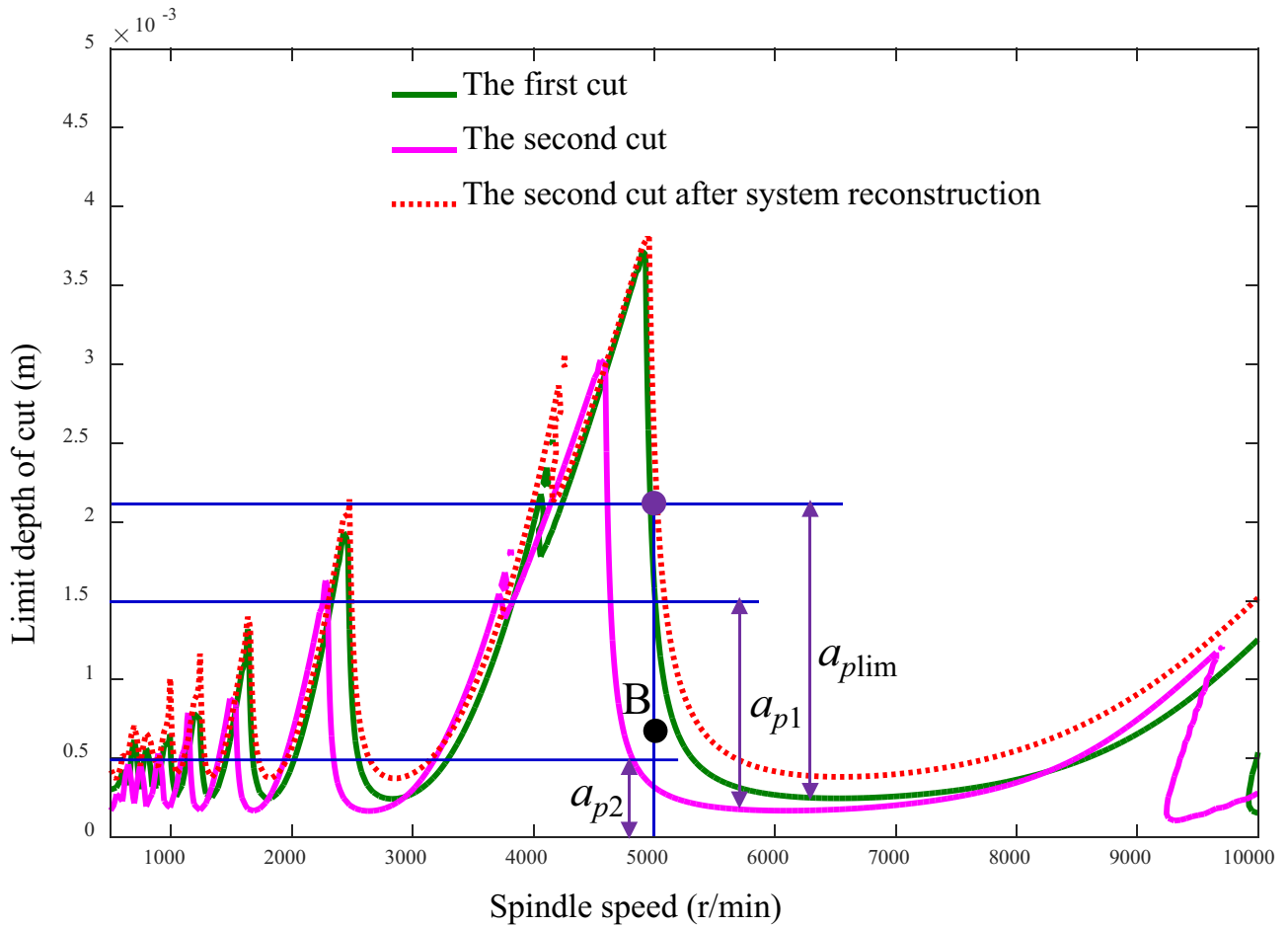


Fig. 13 Stability diagram lobes before and after dynamic characteristic reconstruction

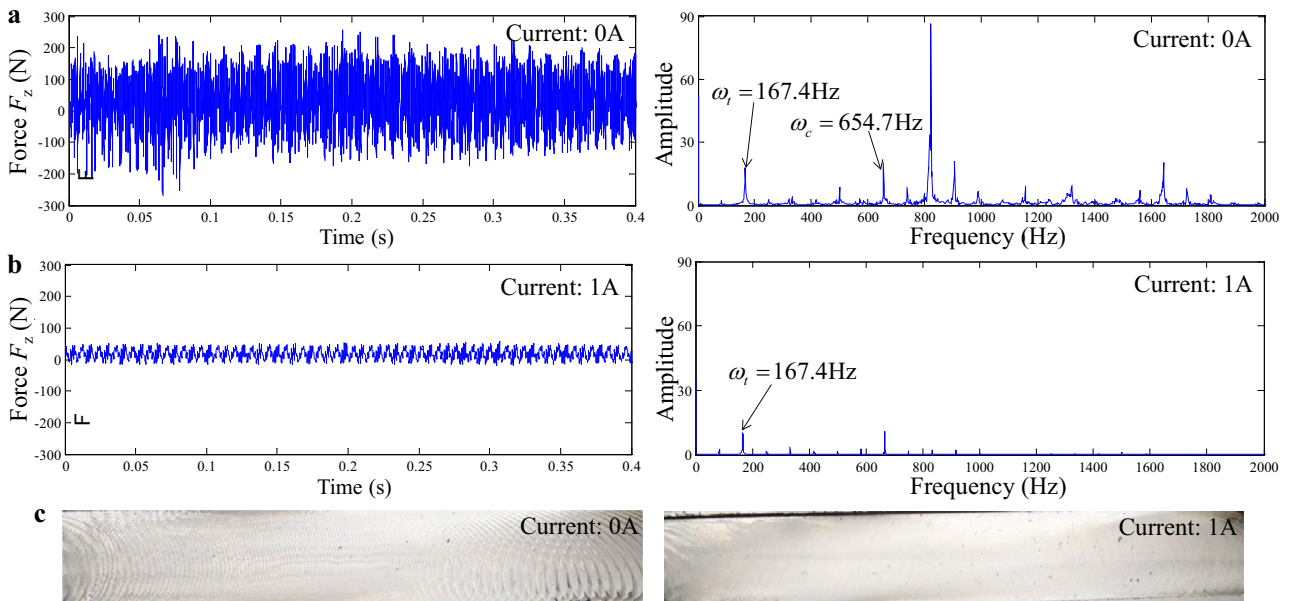


Fig. 14 Cutting force and its spectrum and machined surface before and after fixture-workpiece system reconstruction. **a** z -direction cutting force and its spectrum in the second cut; **b** z -direction cutting

force and its spectrum in the second cut after system reconstruction; **c** machined surface during the second cutting before and after fixture-workpiece system reconstruction

5 Conclusion

MR damping fixture has controllable damping and stiffness characteristics, which can reconstruct the dynamic characteristics of the thin-walled workpiece-fixture system without changing the original fixture layout. Therefore, to realize the milling system dynamic characteristics reconstruction, an active control method based on a MR damping fixture is proposed, and the feasibility and efficiency of the proposed method are validated by experiments. Then, the critical conclusions were drawn from this work as follows:

1. Compared with the conventional methods of process parameters optimization and uncontrollable process stiffness enhancement for suppressing machining vibration, the MR dampers in the fixture can regulate the local damping and stiffness characteristics of the thin-walled workpiece under the determined cutting process parameters and fixture layout. Then, the dynamic characteristics reconstruction scheme of MR damping support fixture-workpiece system is proposed, which is used to improve the system dynamic characteristics of the machining system considering material removal.
2. Based on the stability prediction model found, the fixture-workpiece system dynamic characteristics reconstruction model is established, the time-varying modal parameters in different conditions are iteratively identified, and the stable depth of cut is obtained at any moment. Based on this, the control currents of the MR damping fixture are calculated to offset the change of the damping and stiffness properties caused by material removal in milling.
3. The feasibility and effectiveness of the proposed method are verified by modal and machining tests with different control currents. Experimental results reveal that the dynamic properties of the fixture-workpiece system are improved by regulating the MR damping support fixture, and after the dynamic characteristics of the fixture-workpiece system are reconstructed, the acceleration values and the dynamic cutting force in milling are reduced obviously, and the vibration is suppressed effectively.

Author contribution Junjin Ma: conceptualization, methodology, formal analysis, investigation, and writing—original draft; Yunfei Li: data curation, experimental verification, methodology, and investigation; Dinghua Zhang: writing—review and editing and supervision; Bo Zhao: validation, writing—review and editing and supervision; Xiaoyan Pang: data processing, visualization, and investigation.

Funding This work was co-supported by the National Natural Science Foundation of China (no. 52005166), the Postdoctoral Research Foundation of China (no. 2019M652534), the Henan Postdoctoral Foundation (no. 19030071), the Foundation of Henan Educational Committee (no. 20A460016), the Young Backbone Teachers Foundation Scheme of Henan Polytechnic University (no. 2019XQG-01), and the National

Science Fund for Distinguished Young Scholars of Henan Polytechnic University (no. J2022-5).

Availability of data and materials The data that support the findings of this study are available from the corresponding author upon reasonable request.

Code availability The codes that support the findings of this study are available from the corresponding author upon reasonable request.

Declarations

Ethics approval Not applicable.

Consent to participate All authors agree to participate.

Consent for publication All authors agree to publish.

Conflict of interest The authors declare no competing interests.

References

1. Jiang SL, Sun YW (2020) Stability analysis for a milling system considering multi-point-contact cross-axis mode coupling and cutter run-out effects. *Mech Syst Signal Pr* 141:106452. <https://doi.org/10.1016/j.ymssp.2019.106452>
2. Wu G, Li GX, Pan WC, Raja I, Wang X, Ding SL (2021) A state-of-art review on chatter and geometric errors in thin-wall machining processes. *J Manuf Process* 68:454–480. <https://doi.org/10.1016/j.jmapro.2021.05.055>
3. Zhu LD, Liu CF (2020) Recent progress of chatter prediction, detection and suppression in milling. *Mech Syst Signal Pr* 143:106840. <https://doi.org/10.1016/j.ymssp.2020.106840>
4. Yang Y, Zhang WH, Ma YC, Wan M (2016) Chatter prediction for the peripheral milling of thin-walled workpieces with curved surfaces. *Int J Mach Tools Manuf* 109:36–48. <https://doi.org/10.1016/j.ijmachtools.2016.07.002>
5. Ding Y, Niu JB, Zhu LM, Ding H (2016) Numerical integration method for stability analysis of milling with variable spindle speeds. *J Vib Acoust* 138:011010-1–11011. <https://doi.org/10.1115/1.4031617>
6. Qin CJ, Tao JF, Shi HT, Xiao DY, Li BC, Liu CL (2020) A novel Chebyshev-wavelet-based approach for accurate and fast prediction of milling stability. *Precis Eng* 62:244–255. <https://doi.org/10.1016/j.precisioneng.2019.11.016>
7. Lou WD, Qin GH, Zuo DW (2021) Investigation on Cotes-formula-based prediction method and its experimental verification of milling stability. *J Manuf Process* 64:1077–1088. <https://doi.org/10.1016/j.jmapro.2021.02.045>
8. Dong XF, Qiu ZZ (2020) Stability analysis in milling process based on updated numerical integration method. *Mech Syst Signal Pr* 137:106435. <https://doi.org/10.1016/j.ymssp.2019.106435>
9. Li WT, Wang LP, Yu G (2020) An accurate and fast milling stability prediction approach based on the Newton-Cotes rules. *Int J Mech Sci* 177:105469. <https://doi.org/10.1016/j.ijmecsci.2020.105469>
10. Shi JH, Song QH, Liu ZQ, Ai X (2017) A novel stability prediction approach for thin-walled component milling considering material removing process. *Chinese J Aeronaut* 30(5):1789–1798. <https://doi.org/10.1016/j.cja.2017.05.011>

11. Namazi M, Altintas Y, Abe T, Rajapakse N (2007) Modeling and identification of tool holder-spindle interface dynamics. *Int J Mach Tools Manuf* 47(9):1333–1341. <https://doi.org/10.1016/j.ijmachtools.2006.08.003>
12. Luo M, Zhang DH, Wu BH, Zhou X (2011) Material removal process optimization for milling of flexible workpiece considering machining stability. *P I Mech Eng B-J Eng* 225(8):1263–1272. <https://doi.org/10.1177/2041297510393650>
13. Mori K, Kono D, Yamaji I, Matssubara A (2017) Modelling of viscoelastic damper support for reduction in low frequency residual vibration in machine tools. *Precis Eng* 50:313–319. <https://doi.org/10.1016/j.precisioneng.2017.06.004>
14. Fei JX, Lin B, Xiao JL, Ding M, Yan S, Zhang XF, Zhang J (2018) Investigation of moving fixture on deformation suppression during milling process of thin-walled structures. *J Manuf Process* 32:403–411. <https://doi.org/10.1016/j.jmapro.2018.03.011>
15. Craig O, Picavea J, Gameros A, Axinte D, Lowth S (2020) Conformable fixture systems with flexure pins for improved workpiece damping. *J Manuf Process* 50:638–652. <https://doi.org/10.1016/j.jmapro.2019.12.045>
16. Matsubara A, Taniyama Y, Wang J, Kono D (2017) Design of a support system with a pivot mechanism for suppressing vibrations in thin-wall milling. *CIRP Ann* 66(1):381–384. <https://doi.org/10.1016/j.cirp.2017.04.055>
17. Wang T, Zha J, Jia Q, Chen YL (2016) Application of low-melting alloy in the fixture for machining aeronautical thin-walled component. *Int J Adv Manuf Technol* 87(9–12):2797–2807. <https://doi.org/10.1007/s00170-016-8654-9>
18. Möhring HC, Wiederkehr P (2016) Intelligent fixtures for high performance machining. *Procedia CIRP* 46:383–390. <https://doi.org/10.1016/j.procir.2016.04.042>
19. Wang CX, Zhang XW, Liu YL, Cao HR, Chen XF (2018) Stiffness variation method for milling chatter suppression via piezoelectric stack actuators. *Int J Mach Tools Manuf* 124:53–66. <https://doi.org/10.1016/j.ijmachtools.2017.10.002>
20. Wan SK, Li XH, Su WJ, Yuan JP, Hong J, Jin XL (2019) Active damping of milling chatter vibration via a novel spindle system with an integrated electromagnetic actuator. *Precis Eng* 57:203–210. <https://doi.org/10.1016/j.precisioneng.2019.04.007>
21. Papastathis TN, Ratchev SM, Popov AA (2012) Dynamics model of active fixturing systems for thin-walled parts under moving loads. *Int J Adv Manuf Technol* 62(9–12):1233–1247. <https://doi.org/10.1007/s00170-011-3868-3>
22. Parus A, Powalka B, Marchelek K, Domek S, Hoffmann M (2013) Active vibration control in milling flexible workpieces. *J Vib Control* 19(7):1103–1120. <https://doi.org/10.1177/1077546312442097>
23. Ransom T, Honeycutt A, Schmitz T (2016) A new tunable dynamics platform for milling experiments. *Precis Eng* 44:252–256. <https://doi.org/10.1016/j.precisioneng.2016.01.005>
24. Greiner-Petter C, Tan AS, Sattel T (2014) A semi-active magnetorheological fluid mechanism with variable stiffness and damping. *Smart Mater Struct* 23(11):115008. <https://doi.org/10.1088/0964-1726/23/11/115008>
25. Moradi H, Bakhtiari-Nejad F, Movahhedy MR, Vossoughi G (2012) Stability improvement and regenerative chatter suppression in nonlinear milling process via tunable vibration absorber. *J Sound Vib* 331(21):4668–4690. <https://doi.org/10.1016/j.jsv.2012.05.032>
26. Moradi H, Vossoughi G, Behzad M, Mohammad MR (2015) Vibration absorber design to suppress regenerative chatter in nonlinear milling process: application for machining of cantilever plates. *Appl Math Model* 39(2):600–620. <https://doi.org/10.1016/j.apm.2014.06.010>
27. Ma JJ, Zhang DH, Wu BH, Luo M, Chen B (2016) Vibration suppression of thin-walled workpiece machining considering external damping properties based on magnetorheological fluids flexible fixture. *Chinese J Aeronaut* 29(4):1074–1083. <https://doi.org/10.1016/j.cja.2016.04.017>
28. Guo WC, Zhang Y, Jiang XH, Yang N, Wu K, Liu XA (2021) Improvement of stiffness during milling thin-walled workpiece based on mechanical/magnetorheological composite clamping. *J Manuf Process* 68:1047–1059. <https://doi.org/10.1016/j.jmapro.2021.06.039>
29. Altintas Y (2020) *Manufacturing automation: metal cutting mechanics, machine tool vibration, and CNC Design*. 2nd ed. Cambridge, USA
30. Zhou X, Zhang DH, Luo M, Wu BH (2015) Chatter stability prediction in four-axis milling of aero-engine casings with bull-nose end mill. *Chinese J Aeronaut* 28(6):1766–1773. <https://doi.org/10.1016/j.cja.2015.06.001>

Publisher's Note Springer Nature remains neutral with regard to jurisdictional claims in published maps and institutional affiliations.

Springer Nature or its licensor holds exclusive rights to this article under a publishing agreement with the author(s) or other rightsholder(s); author self-archiving of the accepted manuscript version of this article is solely governed by the terms of such publishing agreement and applicable law.